Applied Energy Symposium 2021: Low carbon cities and urban energy systems
September 4-8, 2021, Matsue, Japan
Paper ID: 49

Optimal thermal match for internal and external cooling water cycles in data server cooling system

Wei He[1,*], Jifang Zhang[1], Chenchen Pei, Xinqiao Wang, Hailong Li, Baoyin Lv

[1]Tianjin Key Laboratory of Refrigeration Technology, Tianjin University of Commerce, Tianjin 300134, PR China
*Correspondence: weihe@tjcu.edu.cn; Tel.: +86-15122779808

ABSTRACT

With the development of data centers for high heat flux, the energy consumption of cooling systems has gradually increased. Introducing an optimal thermal management method for water operation parameters is important for energy saving, but there is a lack of research on this topic. This study focuses on the optimal match for internal and external cooling water operation parameters based on the demand for low energy consumption using TRNSYS simulation software. The relationships among the primary cooling water flow rate, the secondary cooling water flow rate, the cabinet inlet water temperature, and the water supply temperatures of the chiller are explored based on a 4.8 kW data server water cooling system equipped with an air-cooled chiller and a fin-type heat sink, and assuming a safe chip temperature of 70 ℃ and an environmental temperature of 20 ℃. Finally, the optimal performance of the internal and external water cycles were obtained by minimizing the cooling power consumption. The fitting curve of the optimal parameters is provided to improve the design of a low-energy consumption system. In addition, a high chiller water supply temperature is recommended; when the water supply temperature increases from 6 ℃ to 16 ℃, the total power consumption can be reduced by 14%.

Keywords: Data center, Power consumption, Water chiller, Thermal management

1. INTRODUCTION

With the construction of the information superhighway, the demand for data storage, reading, and data analysis in various industries has increased rapidly. In addition, with the high integration of electronic components (such as CPU chips), the heat flux of data centers increases linearly; moreover, the main heat generation components are the CPU chips. To ensure that the operating temperature of chips is within a safe range, the thermal management of data centers is required, in which an efficient cooling system becomes an important challenge to consider [1].The cooling system of the data center is mainly used to collect heat and transfer it to the external environment; however, the power consumption of the cooling system accounts for 40% of the total power consumption of the data center [2]. Therefore, it is necessary to design and develop an efficient cooling system to reduce energy consumption while reducing the heat of the chip.

Generally, a reliable and mature air cooling method is adopted for data centers. However, with the increasing heat flux trend, the air cooling method does not meet the cooling demand. Consequently, liquid cooling methods have attracted considerable attention from researchers in recent years [3]. The liquid cooling is attributed to two factors: the internal heat dissipation of the server cabinet and the external cold source. For internal heat dissipation research, it is best to optimize the heat sink in the data center server. Maajej [4] and Zhu [5] adopted a finned air-cooled tube system and annular heat pipe, respectively. Minking [6] studied the influence of the height of the pine-fin array on heat transfer performance. Leng [7] designed a double-layer microchannel radiator and optimized the variables of temperature uniformity and thermal resistance of the bottom wall. Shwaish [8] and Jajja [9] studied the influence of fin height and fin spacing on heat dissipation performance. Kumar [10] reported the

Selection and peer-review under responsibility of the scientific committee of CUE2021

effects of fin height, fin thickness and inlet Angle on the cooling capacity of the radiator. For the external cold source research, it is focused on using various cold sources to improve the cooling efficiency. Kanbur [11] introduced single-phase and two-phase immersion cooling systems. Levin [12] designed a liquid immersion server and considered the structure, layout, and technical characteristics of a liquid immersion cooling system. Zhang [13] developed four typical free cooling systems. Yang [14] provided hybrid cold source operating modes by switching the traditional mechanical refrigeration mode, part of the free cooling mode, and all free cooling modes according to different outdoor temperatures. Zhang [15] introduced an integrated cooling system for mechanical refrigeration and thermosiphons.

Through a literature review, we found that there is no relevant research on parameter optimization or the matching analysis of the internal server cooling cycle as well as the external cooling source cycle in a liquid cooling system. The performance of the heat sink directly affects the parameters in the server cooling cycle. Therefore, when the energy consumption analysis is conducted, it is reasonable to include the radiator type, cold source, internal server cooling cycle, and external cooling source cycle into the energy consumption analysis of the entire cooling system. To study the optimal thermal management of the internal server cooling cycle and the external cold water cycle, we simulated the working conditions of the internal and external cooling cycles based on the minimum energy consumption. The cooling system consists of an external chiller and a finned heat sink for internal server cooling. Finally, the optimization parameters are introduced in the design of the data center to ensure the safe operation of the CPU chip with the lowest power consumption.

2. METHODOLOGY

2.1 System construction and modeling

A data center cooling system consisting of a server cabinet with total 4.8 kW load and a water cooling system with air-cooled chiller taken. The server cabinet includes 12 chips of each has a thermal power of 400 W. and the water-cooled fin-type heat sink is located on the top of each chip. The system equipment and coupled water circulations are shown in Fig. 1(a). Two water cycles were connected by a plate-type heat exchanger in a countercurrent manner. The water on the side of the air-cooled chiller was called primary cooling water (run by Pump-1), while the water on the side of the server cabinet (run by Pump-2) is called secondary cooling water. The q_{v1}, q_{v2}, T_{server}, *and* $T_{chiller}$ denote the primary water flow rate, secondary water flow rate, water inlet temperature of the server, and water supply temperature of the chiller, respectively. The fin-type water-cooled heat sink structure is shown in Fig.1(b), where, L_b=115 mm, W_b=78 mm, and H_b=3 mm refer to the length, width, and height of the bottom plate, respectively. L_f =72.6 mm, W_f =0.8 mm, H_f =3.5 mm, and S_f =0.45 mm express the length, width, height of one fin, and the space between two fins, respectively.

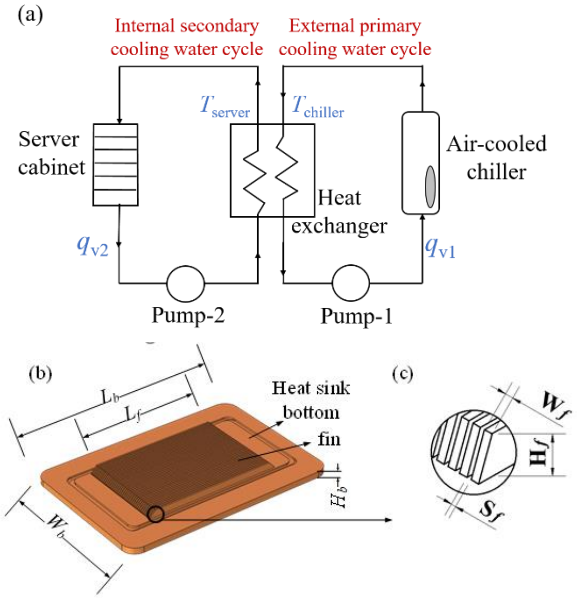

Fig. 1 Schematic of data center cooling system, (a) system equipment and coupled water circulations, (b) fin-type water-cooled heat sink structure.

2.1.1 *Heat dissipation model of heat sink*

According to Fourier's law, for a one-chip water-cooling unit, the chip temperature can be expressed by the following equation:

$$T_{chip} = T_f + Q \cdot R_{total} \quad (1)$$

where R_{total} (K W^{-1}) is the total thermal resistance, *and* Q (kW) denotes the thermal power from one chip, which is a constant value of 400 W in this study. T_f (°C) represents the average temperature of the fluid.

Furthermore, according to the heat transfer mechanism, the total thermal resistance between the coolant and hot chip can be classified as follows: the contact thermal resistance R_{cont} (K W^{-1}), which appears at the interface surface between the heat sink plate and chip; conduction thermal resistance R_{cond} (K W^{-1}), which appears in the heat sink plate; and convection thermal

resistance R_{conv} (K W^{-1}) caused by water fluid flow. Therefore, R_{total} can be calculated as follows:

$$R_{total} = R_{cont} + R_{cond} + R_{conv} \quad (2)$$

The three thermal resistances are calculated by the following equations:

(I) The contact resistance R_{cont}:

$$R_{cont} = \delta_s \Big/ \left\{ L_f \left[(n-1) S_f + n * W_f \right] \lambda_s \right\} \quad (3)$$

where n is the number of fins in one heat sink, which in our case it is 38; δ_s (mm) and λ_s (W m^{-1} K^{-1}) are the thickness and thermal conductivity of the thermal grease, respectively. The constant values of 1.5 mm and 4.5 W m^{-1} K^{-1} [16] are employed for the thickness and thermal conductivity, respectively.

(II) The conductivity resistance R_{cond}:

$$R_{cond} = H_b \Big/ \left(W_b L_b \lambda_c \right) \quad (4)$$

where λ_c=400 W m^{-1} K^{-1} is applied as the thermal conductivity of copper.

(III) The convection resistance R_{conv}:

$$R_{conv} = 1 \Big/ \left\{ h \left[L_f S_f (n-1) + 2\eta_f L_f H_f (n-1) \right] \right\} \quad (5)$$

where h is the heat transfer coefficient when water flows through the heat sink, and η_f is the fin efficiency.

2.1.2 Power consumption model of cooling system

To calculate and compare the cooling system efficiency, the power consumed by the IT equipment and cooling system was considered as the total power consumption. Other parts power consumptions, such as power supply, distribution, and auxiliary equipment were excluded. Therefore, the power usage effectiveness (PUE) was applied to evaluate the air conditioning system in a data center as follows [17]:

$$P_{system} = P_{chiller} + P_{pump1} + P_{pump2} \quad (6)$$

$$\mathrm{PUE} = \left(P_{IT} + P_{system} \right) / P_{IT} \quad (7)$$

where P_{system} denotes the total power consumption of the cooling systems, and P_{IT} refers to the power consumption of the IT equipment. $P_{chiller}$, P_{pump1}, and P_{pump2} contribute to the power consumption of the chiller, power consumption of Pump-1, and power consumption of Pump-2, respectively.

TRNSYS was applied to calculate the power consumption in the entire cooling system under various working conditions. A constant load of 4.8 kW was input into the model. The inlet and outlet temperatures and the power consumed by each equipment could be calculated by the temperature modules and power consumption modules in the software automatically by inputting the equipment and fluid parameters.

2.2 Simulation validation

An experiment test was built, and the experimental and simulation results were compared at an ambient temperature of 18 °C and a thermal chip power of 200 W, as summarized in Table 1. The flow rates of the secondary and primary cooling water were 5.35 and 7.83 L/min, respectively. The relative errors of the chip temperature and system power consumption between the experimental and simulated values were 5.64% and 3.13%, respectively. During the experiment, the heat generated by the chip was not completely absorbed by the heat sink, and some of it was exchanged with the environment. Therefore, the experimental power consumption of the water-cooling system was lower than the simulated value. The contact thermal resistance between the bottom plate of the radiator and the chip was relatively larger than the ideal thermal resistance used in the simulation, leading to a higher experimental cooled temperature of the chip. Therefore, the current simulation models were validated for the numerical evaluation and experimental data are in good agreement.

Table 1 Comparison of experimental and simulation results.

Parameter	Experimental value	Simulated value	Relative error
Chip temperature	69.2 °C	65.3 °C	5.64%
System power consumption	0.93 kW	0.96 kW	3.13%

3. RESULTS AND DISCUSSION

To maintain the operating temperature of the chip within the safe range, cooling water is required to remove the heat generated over time. A relationship potentially exists among all the cooling water operation parameters, including the primary cooling water flow rate (q_{v1}), secondary cooling water flow rate (q_{v2}), cabinet inlet water temperature (T_{server}), and the water supply temperature of the chiller ($T_{chiller}$). Given the required safe chip temperature is 70 °C and the ambient temperature is 20 °C, the energy consumption of the cooling water system under different water operation conditions is studied in this section.

Fig. 2 shows the variation in the cooling water flow rates with the cabinet inlet water temperature at different temperatures of the chiller. Therefore, to maintain the chip working at 70 °C, the required secondary cooling water flow rate is only determined by the cabinet inlet water temperature. The secondary

cooling water flow rate gradually increases with an increase in the cabinet inlet water temperature. The required primary cooling water flow rate is determined by both the cabinet inlet water temperature and the water supply temperature of the chiller. By maintaining the water supply temperature of the chiller constant, the primary cooling water flow rate changes with the inlet water temperature of the cabinet, first by decreasing and then increasing. By maintaining the inlet water temperature of the cabinet constant, the higher the water supply temperature of the chiller, the higher the primary cooling water flow rate. Generally, the cabinet inlet water temperature has a clearer effect on the required secondary cooling water flow rate than the required primary cooling water flow rate. Different cooling water flow rates lead to different values of power consumption in the pump. The corresponding primary and secondary pump power consumption values are shown in Fig. 3. From this, the change in the trend of the pump power consumption with the cabinet inlet water temperature and water supply temperature of the chiller is consistent with the change in the water flow rate, as shown in Fig. 2. The smaller the water flow rate, the smaller the pump power.

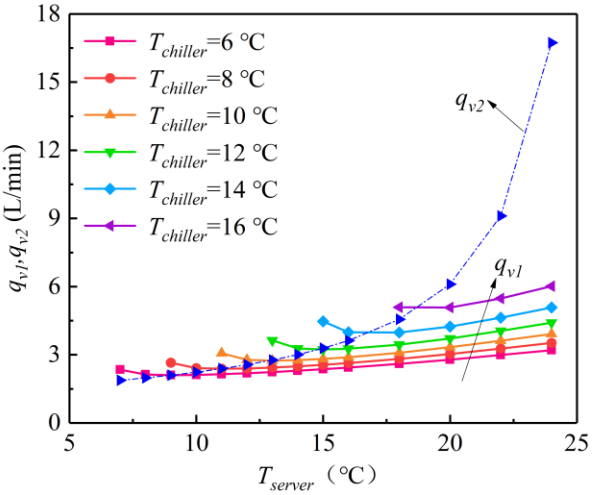

FIG. 2 Change in the cooling water flow with cabinet inlet water temperature and water supply temperature of chiller

In addition to the pump power consumption, the chiller power consumption is another key factor in cooling water systems. Fig. 4 shows the power consumption of the chiller corresponding to the changing temperature of the server. When the water supply temperature of the chiller remains constant, the chiller power consumption is unaffected by the change in the inlet water temperature of the cabinet. When the inlet water temperature of the cabinet remains unchanged, the power consumption of the chiller decreases significantly with an increase in the water supply temperature of the chiller. However, as shown in Fig. 2, the required primary water flow rate increases with an increase in the water supply temperature of the chiller, thus leading to an increase in the primary pump power consumption. Therefore, increasing the chiller supply water temperature can lead to low chiller power consumption and a high primary cooling water flow rate.

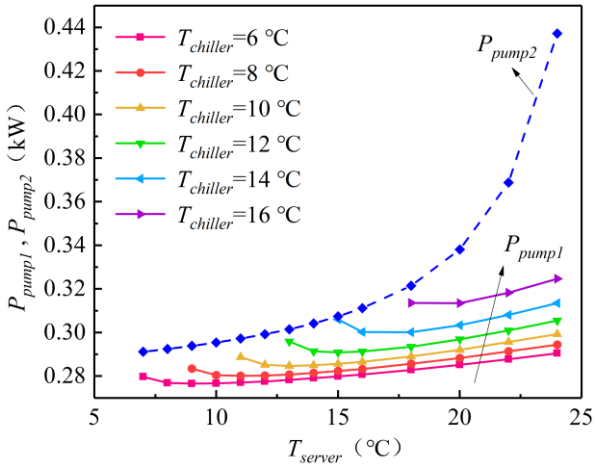

FIG. 3 Change in the pump power consumption with cabinet inlet water temperature and water supply temperature of chiller

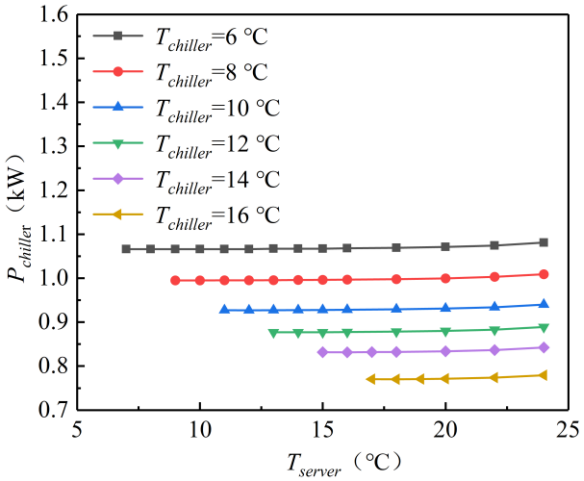

FIG. 4 Change in the chiller power consumptions with cabinet inlet water temperature and water supply temperature of chiller

We explored the optimal water operation conditions to achieve minimum total energy consumption. Basing on it, Fig. 5 shows the total power consumption of the cooling water system under different water working conditions. Through comparison, it was found that with the increase in the inlet water temperature of the cabinet, the total power consumption first decreases and then increases. The optimal water operation parameters are obtained at the minimum power consumption point, which are

marked by circles in Fig. 5. Taking the 12 ℃ case of the chiller temperature, when the minimum power consumption ($P_{system,min}$) is obtained, the optimal inlet water temperature of the cabinet is $T_{sever,opt}$=14 ℃, where the optimal primary water flow rate is $q_{v1,opt}$=3.3 L/min and the optimal secondary water flow rate is $q_{v2,opt}$=3 L/min, as shown in Fig. 1. There are different optimal inlet water temperatures of the cabinet for different water supply temperatures of the chiller, and the higher the chiller supply water temperature, the higher the optimal inlet water temperature of the cabinet. In addition, the total power consumption decreases with an increase in the water supply temperature of the chiller when the inlet water temperature of the cabinet is constant.

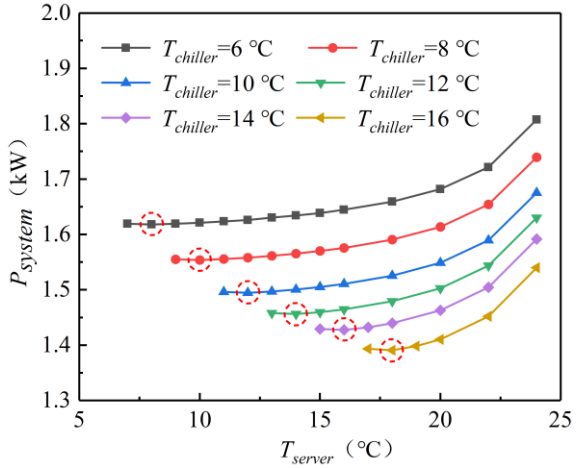

FIG. 5 Change in the total system power consumptions with cabinet inlet water temperature and water supply temperature of chiller

Based on the above analysis, the optimal cabinet inlet water temperature and optimal water flow rates corresponding to different water supply temperatures of the chiller can be obtained, as shown in Fig. 6. From this, with an increase in the water supply temperature of the chiller, the optimal cooling water flow increases nonlinearly whereas the optimal cabinet inlet water temperature increases linearly. Fitting the curve can improve the design of an optimal cooling system with low energy consumption.

When considering the optimal operation parameters, as shown in Fig. 6, the corresponding minimized energy consumption and PUE of the cooling system are shown in Fig. 7. As shown, both the primary and secondary pump power consumptions are approximately 0.3 kW, but the chiller power consumption is approximately 0.9 kW. With an increase in the water supply temperature of the chiller, the power consumption of the cooling pump increases slightly, but the power consumption of the chiller decreases significantly. Finally, the total power consumption and PUE increases with an increase in the water supply temperature of the chiller. Therefore, increasing the water supply temperature of the chiller is optimal for energy saving in cooling systems. When the water supply temperature increases from 6 ℃ to 16 ℃, the total power consumption and PUE is reduced by 14% and 4%, respectively.

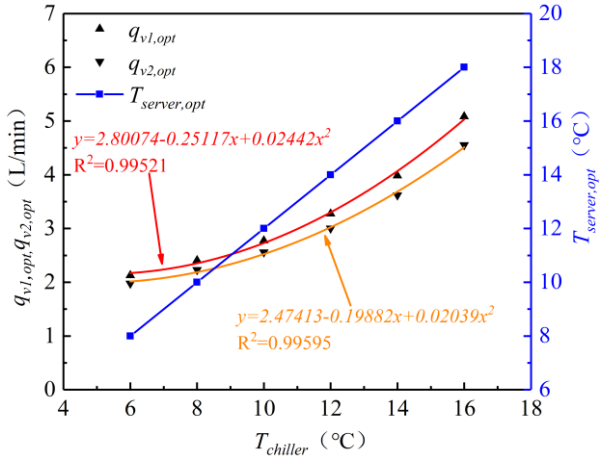

FIG. 6 Optimal cooling water flow rate and optimal cabinet inlet water temperature change under different water supply temperatures of the chiller

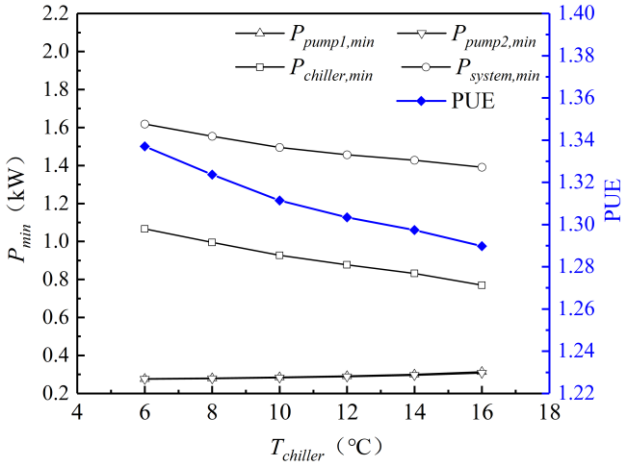

FIG. 7 Minimized energy consumption and PUE changes under different water supply temperatures of the chiller

4. CONCLUSION

By considering a safe chip temperature of 70 ℃ and an environment temperature of 20 ℃ as the case, the energy consumption of the data server's cooling system was analyzed for different water working conditions.

First, to meet the chip temperature, the required secondary cooling water flow rate was determined by

the cabinet inlet water temperature. However, the required primary cooling water flow rate was determined by both the cabinet inlet water temperature and the water supply temperature of the chiller. Furthermore, a relationship between water temperature and the flow rate was determined.

Second, based on the above relationships, the optimal inlet water temperature of the cabinet and optimal water flow rates exist corresponding to the minimum total power consumption for a given water supply temperature of the chiller. The optimal cooling water flow rate increases nonlinearly, and the optimal cabinet inlet water temperature increases linearly with an increase in the chiller supply temperature. The fitting curve of the optimal parameters is provided to improve the design of a low-energy consumption system.

Third, it is recommended to choose or develop a chiller with a high water supply temperature that can achieve significant energy savings on the cooling system of the data center. When the water supply temperature increases from 6 °C to 16 °C, the total power consumption can be reduced by 14%.

ACKNOWLEDGEMENT

The authors are grateful for financial support from Tianjin Natural Science Foundation (No.18JCZDJC97100), the National Natural Science Foundation of China (51806152) and the International Cooperation Program of the Ministry of Science and Technology of China (2017YFE0198000).

REFERENCE

[1] Chen H, Peng Y hang, Wang Y ling. Thermodynamic analysis of hybrid cooling system integrated with waste heat reusing and peak load shifting for data center. Energy Convers Manag 2019;183:427–39.

[2] Carbó A, Oró E, Salom J, Canuto M, Macías M, Guitart J. Experimental and numerical analysis for potential heat reuse in liquid cooled data centres. Energy Convers Manag 2016;112:135–45.

[3] Haywood AM, Sherbeck J, Phelan P, Varsamopoulos G, Gupta SKS. The relationship among CPU utilization, temperature, and thermal power for waste heat utilization. Energy Convers Manag 2015;95:297–303.

[4] Maalej S, Zayoud A, Abdelaziz I, Saad I, Zaghdoudi MC. Thermal performance of finned heat pipe system for Central Processing Unit cooling. Energy Convers Manag 2020;218:112977.

[5] Zhu K, Chen XQ, Dai BM, Zheng MZ, Wang YB, Li HL. Operation characteristics of a new-type loop heat pipe (LHP) with wick separated from heating surface in the evaporator.Appl Therm Eng 2017;17.

[6] Chyu MK, Siw SC. Effects of height-to-diameter ratio of pin element on heat transfer from staggered pin-fin arrays. ASME Turbo Expo 2009: Power for Land, Sea, and Air 2016;1–9.

[7] Leng C, Wang XD, Wang TH, Yan WM. Optimization of thermal resistance and bottom wall temperature uniformity for double-layered microchannel heat sink. Energy Convers Manag 2015;93:141–50.

[8] Plate S, Heat FIN. Thermal / Fluid Performance Evaluation of 2002:267–75.

[9] Ayub S, Ali W, Maryam A. Water cooled minichannel heat sinks for microprocessor cooling : Effect of fi n spacing 2014;64:76–82.

[10] Kumar S, Singh PK. International Journal of Thermal Sciences E ff ects of fl ow inlet angle on fl ow maldistribution and thermal performance of water cooled mini-channel heat sink. Int J Therm Sci 2019;138:504–11.

[11] Kanbur BB, Wu C, Fan S, Duan F. System-level experimental investigations of the direct immersion cooling data center units with thermodynamic and thermoeconomic assessments. Energy 2021;217:119373.

[12] Levin II, Dordopulo AI, Doronchenko YI, Raskladkin MK, Fedorov AM, Kalyaev Z V. Immersion liquid cooling FPGA-based reconfigurable computer system. IFAC-PapersOnLine 2016;49:366–71.

[13] Zhang Y, Wei ZY, Zhang MS. Free cooling technologies for data centers: energy saving mechanism and applications. Energy Procedia 2017;143:410-15.

[14] Yang Y, Wang B, Zhou QB. Energy saving analysis of free cooling system in the data center. Procedia Engineering 2017;205:1815-19.

[15] Zhang HN, Shao SQ, Tian CQ. Simulation of the thermosyphon free cooling mode in an integrated system of mechanical refrigeration and thermosyphon for data centers. Energy Procedia 2015;75:1458-63.

[16] Gwinn J P, Web RL, Performance and testing of thermal interface materials. Microelectron J 2003;34:215-22.

[17] Malone C, Belady C. Metrics to characterize data center & IT equipment energy use. Proceesdings of 2006 Digital Power Forum: Richardson TX 2006.